INVESTIGATION OF THE INFLUENCE OF THE WELDING SPEED AND CURRENT ON THE PARAMETERS OF THE ADAPTIVE FUNCTION

M. B. NASIRI*, A. PUTZ* and N. ENZINGER*

** Institute of Materials Science, Joining and Forming, Graz University of Technology, Graz 8010, Austria, Email: Mohammad.nasiri@tugraz.at*

DOI 10.3217/978-3-85125-615-4-44

ABSTRACT

The adaptive function developed by authors allows direct correlation between welding circumstances and temperature distribution using limited experimental data including weld pool dimensions and temperature at some arbitrary points. This paper intends to investigate the effects of welding speed and welding current on the parameters of the adaptive function. GTAW with various welding speeds and various welding currents was applied on duplex stainless steel plates. According to the experimental data, the parameters of the adaptive function were expressed as a function of welding speed and weld pool dimensions. To show the effectiveness of the new method, Rosenthal model and FEM were employed to simulate the conducted welding and the accuracy of the predicted result rather than the measured temperature were estimated by relative error. The results show that the adaptive function method is more accurate than the FEM and Rosenthal approach in all studied cases.

Keywords: Welding Simulation, Heat Flow, Analytical Solution, Partial Differential Equation, FEM

INTRODUCTION

Modelling and simulation of the thermal cycle and the subsequent mechanical behaviours have been investigated for more than 80 years. Analytical, numerical and empirical approaches have been employed to solve the heat flow problem in welding [1]. However, the proposed solutions have shown an only limited success. Analytical solutions such as Rosenthal solution are limited by accuracy [2] and numerical solutions are computationally expensive [3]. The adaptive function method (AFM) is based on a mathematical 3D function which can be adjusted using experimental data and it can be used to solve the partial differential equation of any moving heat source with high accuracy and low computation cost [4]. The parameters of the adaptive function are directly determined by temperature measurement and no information about material properties, phase transformation, and heat source parameters are required [4]. Therefore, the adaptive function method is able to overcome the obstacles of inaccuracy and computation cost. This paper intends to study the dependency of the parameters of the adaptive function to the welding speed and welding current and make a correlation between them.

EXPERIMENTAL SETUP

A Gas Tungsten Arc Welding (GTAW) process using argon as shielding gas with various welding speed and welding current given in Table 1 was applied on duplex stainless steel plates with the dimensions given in Table 2 and chemical composition given in Table 3. Tests No. 1-4 were conducted with a same welding current of 150A; and welding speed varies from 7 to 12cm/min. The welding speed was constant for test series No. 2, 5-8 and in this series the welding current differs from 125 to 175 A. The welding parameters of test No. 7 and 8 are same as test No. 5 and 2 respectively but in these cases, the temperature of the bottom surface of the plate were measured instead of the top surface. Experimental data including weld pool dimension and temperatures measured at specified points were extracted to be used in modelling. The temperature history of points at positions shown in Fig. 1, were measured by type K thermocouples (0.3 mm in diameter). After welding the width (W), depth (D), rear tail (L_r) and front radius (L_f) of the weld pool were measured on the samples and are presented in Table 4. Fig. 2 shows the macrograph of the weld bead of the test No. 6.

Table 1 Parameters of the welding process at the constant welding voltage of 14V

Test No.	Welding current (A)	Speed (cm/min)
1	150	7
2		8.4
3		10
4		12
5	125	8.4
6	175	
7	125	
8	150	

Table 2 Dimensions of the welding plate

Plate size (mm)		
Width	length	thickness
100	200	10

Table 3 Chemical composition of the duplex stainless steel 1.4462 plates

Element	C	Mn	P	S	Si	Cu	Cr	Ni	Mo	Nb	N
Weight %	0.026	1.9	0.02	0.007	0.67	0.47	23	5.5	3	0.5	0.2

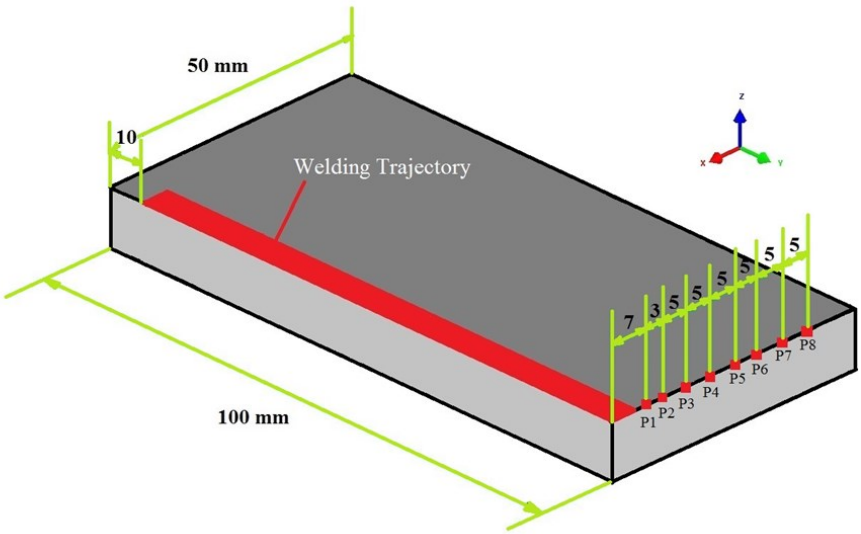

Fig. 1 Schematic of a quarter of the welding plate and the position of the thermocouples which are all in one line

Table 4 Weld pool dimensions (mm)

Test No.	W	L_f	L_r	D
1	4.6	3.8	8.5	2.1
2	4.3	3.3	7.4	1.9
3	4.0	2.8	6.2	1.7
4	3.7	2.3	5.2	1.5
5	3.8	2.8	5.4	1.7
6	5.2	3.8	9.6	2.1
7	3.8	2.8	5.4	1.7
8	4.3	3.3	7.4	1.9

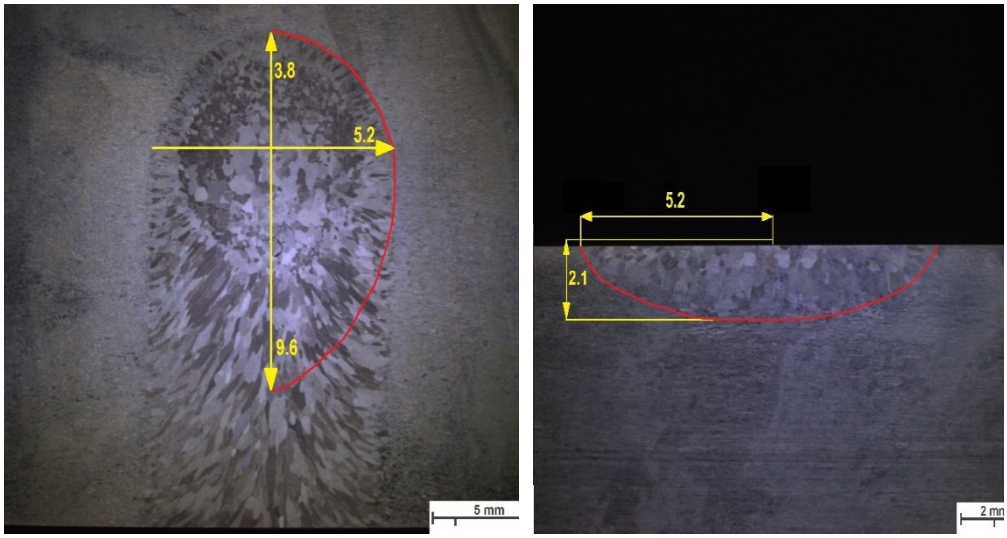

(a) (b)

Fig. 2 Macrograph of the bead of the test No.6 (a) upper view (b) cross section

MODELING METHODS

The conducted welding tests were simulated by Rosenthal's model and FEM beside the AFM to examine the accuracy of the available methods in different welding cases.

ROSENTHAL METHOD

The theory of heat conduction that was developed by Fourier and applied to a moving heat sources by Rosenthal [5] is the most popular and simplified analytical method used to calculate the thermal history of welds. The quasi-steady state solution of Rosenthal using the transformation presented by Eq. 1 for a semi-infinite plate expresses temperature as a function of the position and constant physical properties of the material (Eq. 2) when the point heat source moves along the y-axis. A Matlab routine was developed to calculate the temperature field based on Rosenthal's model. The constant thermo-physical properties of duplex stainless steel were considered according to the Table 5 and the arc thermal efficiency of GTAW was considered to be 0.7 [6].

$$\xi = y - vt \tag{1}$$

$$T = T_0 + \frac{Q}{2\pi kR} e^{\left(-\frac{\rho c v}{2k}(R+\xi)\right)} \tag{2}$$

$$R = \sqrt{x^2 + \xi^2 + z^2} \tag{3}$$

Table 5 Material properties of Duplex stainless steel at room temperature [7], [8]

Heat capacity (J/kg °C)	Density (kg/m2)	Conductivity(J/m)	Melting Point(°C)
495	7990	15	1400

By considering the quasi-steady state condition, the measured temperature history (time-temperature) of a point can be converted into a spatial temperature distribution along the y-axis (y-temperature) using Eq. 1. Accordingly, the temperature distribution along the y-axis at 7, 10, 15, 20, 25, 30, 35 and, 40mm away from the centreline, were calculated according to the recorded temperatures at points P1- P8 (Fig. 1). Fig. 3 shows the result of Rosenthal model for upper surface along with calculated and measured fusion line in x-y cross-sections and the relative errors based on the measured temperature [4]. According to the result, the accuracy of Rosenthal's model is low in the prediction of the weld pool size and the relative error of calculated temperature is between 37-53% in the case of test No.1.

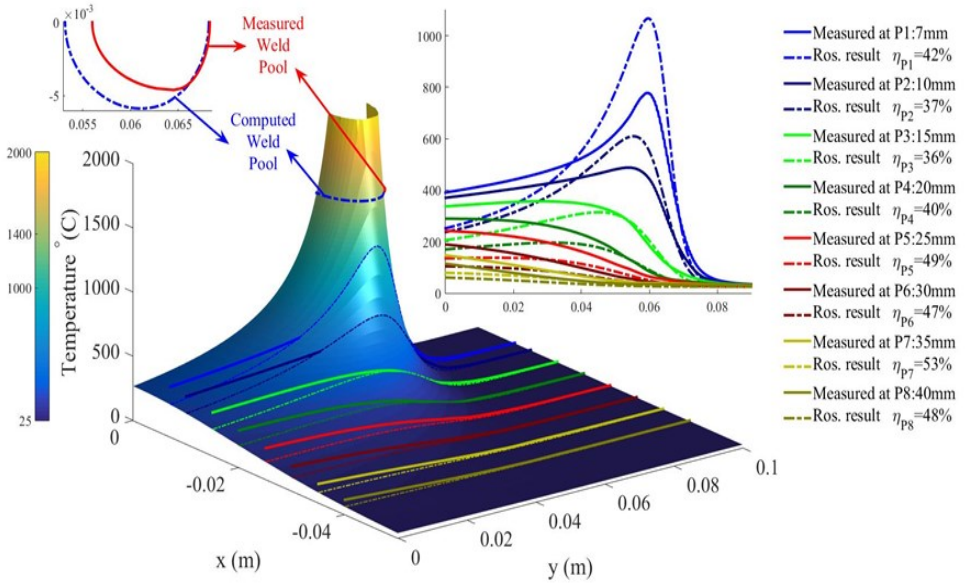

Fig. 3 Temperature distribution on the upper surface of the plate as calculated with the Rosenthal equation for test No. 1(welding speed 7 cm/min, welding current 150A)

FINITE ELEMENT METHOD (FEM)

The thermal fields and the weld pool dimensions of the bead on plate gas tungsten arc welding have been investigated by using SYSWELD, a software package that can be used to conduct numerical analyses of welding processes. The minimum mesh size was

considered 0.5 mm for elements close to the welding trajectory, and 8 mm mesh size was considered as the maximum at the edges of the plate as shown in Fig. 4. The parameters of the double ellipsoidal heat source model are presented in Table 6 and the arc efficiency considered to be 0.7 [6]. The material properties considered to be temperature dependent according to the SYSWELD database. The initial temperature was set at 25°C and heat losses due to convection and radiation were taken into account using SYSWELD database for natural air cooling medium [9].

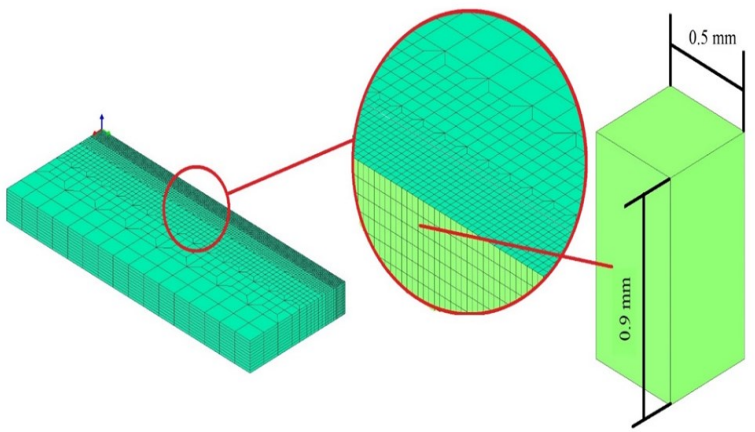

Fig. 4 Half of the FEM model

Table 6 Double ellipsoidal heat source parameters (Goldak's model) [9], [10]

Test No.	Width ($2\times a_w$) (mm)	Length ($b_{hf} + b_{hr}$) (mm)	Penetration (c_w) (mm)	Length Ratio ($\frac{b_{hf}}{b_{hr}}$)	Energy per length ($\frac{J}{mm}$)
1	8.28	11.07	1.98		
2	7.74	9.63	1.71	0.45	1470
3	7.2	8.1	1.53		
4	6.75	6.75	1.35		
5	6.84	7.38	1.53	0.5	1225
6	9	11.92	1.98	0.38	1715
7	6.84	7.38	1.53	0.5	1225
8	7.74	9.63	1.71	0.45	1470

Fig. 5 shows the result of the FEM simulation of test No. 1 on the upper surface and compares the experimental data with the computed result. The relative error of the FEM, in this case, is 12-22% that shows the FEM is almost 58-67% more accurate than the Rosenthal's approach.

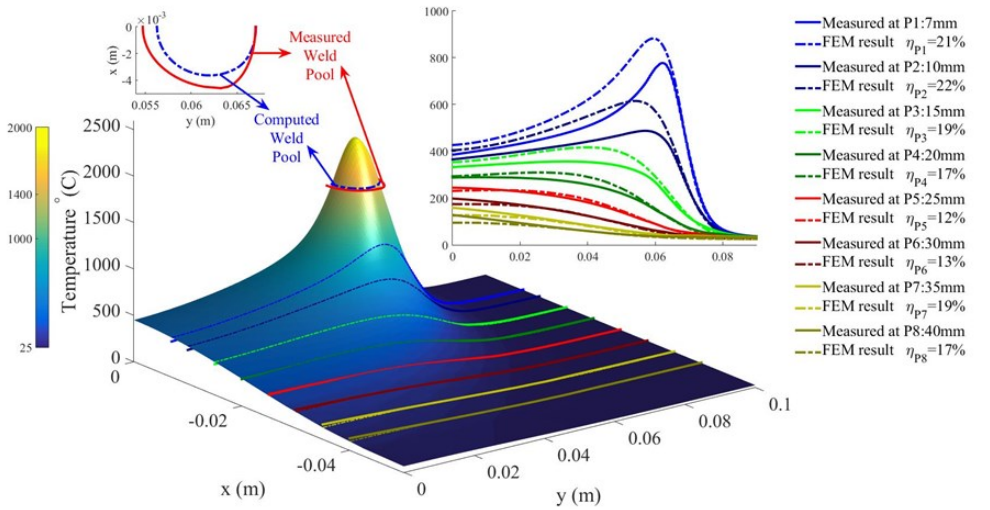

Fig. 5 Temperature distribution on the upper surface of the plate of test No. 1 as calculated with the FEM (welding speed 7 cm/min, welding current 150A)

ADAPTIVE FUNCTION METHOD

The rigid formulation of Eq. 2 does not allow for changes in such a way, that the result can be matched to the measured temperature. The material properties and arc thermal efficiency are just the parameters of the Rosenthal's equations that can be manipulated to increase the accuracy of the Rosenthal's solution. However, the different values of those parameters may improve local accuracy at a point but may destroy accuracy in other places and therefore several researchers tried to modify the Rosenthal's equations which shows limited success [2], [11], [12], [13], [14], and [15]. In the case of the FEM method, the accuracy might increase by considering more accurate heat source model, material properties or boundary conditions which are required more computational and experimental works. High accuracy in the weld pool and its adjacent area can be obtained using a suitable heat source model or manipulating the parameters of the heat source model by trial and error [16]. The material properties which are used in FEM require considering the deconvergence effect of sharp changes in material properties which inhibits accuracy improvement of the FEM [17]. The principle of the adaptive function method is based on a function which can be matched to the measured temperature by determining some limited parameters directly by using experimental data. In fact, the adaptive function method proposes that instead of dealing with mathematical models of the physical phenomena which occur in welding, we can consider the cumulative effects of those phenomena which appear in the form of temperature distribution and weld pool dimensions. The adaptive function is developed by manipulating the Rosenthal equation so that the calculated fusion line coincides with the measurement. Accordingly, the term R (Eq. 3) in the Rosenthal's equation which is the mathematical equation of a sphere is replaced by the equation of an ellipsoid. To coincide with the temperature distribution in the rest of the welding sample with the reality a

modification function is proposed which adjusts the temperature gradient along the main axis. The proposed adaptive function is as follows [4]:

$$T = T_0 + \frac{1}{R_p} e^{(-B(R+y))} \tag{4}$$

$$R_p = \sqrt{\left(f\left(\frac{x}{W}\right) \times \frac{x}{a_m}\right)^2 + \left(f\left(\frac{\xi}{L_f}\right) \times \frac{\xi}{b_m}\right)^2 + \left(f\left(\frac{z}{D}\right) \times \frac{z}{c_m}\right)^2 + {d_m}^2} \quad ;\xi \geq 0 \tag{5}$$

$$R_p = \sqrt{\left(f\left(\frac{x}{W}\right) \times \frac{x}{a_m}\right)^2 + \left(f\left(\frac{\xi}{L_r}\right) \times \frac{\xi}{b_m}\right)^2 + \left(f\left(\frac{z}{D}\right) \times \frac{z}{c_m}\right)^2 + {d_m}^2} \quad ;\xi < 0 \tag{6}$$

$$f(\omega) = \left(M\omega^2 - M\sqrt{\omega^2 + 1}\right)^N \tag{7}$$

The parameters of the adaptive function including a_m, b_m and c_m cause the adaptive function to match the real fusion line. The parameter d_m removes the singularity in the origin of the moving heat source, and it is the main factor which determines the maximum temperature at the origin (centre of the heat source) [4]. By considering the weld pool dimensions and an estimated maximum temperature T_{max} from the experiment, the optimum values of the parameters are determined so that the calculated fusion line coincides with the measurement [4].

The term $\frac{k}{\rho c}$ in Eq. 2 is heat diffusivity which is a temperature-dependent material property in the solid state, while the heat diffusivity in the weld pool strongly depends on the mass transfer. Since it is not possible to consider the temperature dependency of the physical properties and the mass transfer with an analytical equation, the term $\frac{\rho c}{2k} v$ is substituted by a constant value of B as a function of welding speed which is considered to be a parameter of the adaptive function.

$$B = \frac{\rho c}{2k} v \tag{8}$$

The modification function f is a function of dimensionless parameter of ω which changes the scale from a length unit (m) to the scale of the weld pool dimensions. In order to avoid changing the melting isotherm, the modification function $f(\omega)$ is always 1 everywhere along the fusion line, which is defined by Eq. 9.

$$\omega_x = \frac{x}{W} \; ; \; \omega_{\xi f} = \frac{\xi}{L_f}; \; \omega_{\xi r} = \frac{\xi}{L_r} \; ; \omega_z = \frac{z}{D} \tag{9}$$

Fig. 6 shows the result of the FEM for the upper surface of the sample of test No.2. As shown in Fig. 6, welding temperature curves in any cross section parallel to the main axis, have a special waveform shape. The M and N as parameters of the modification function provide the flexibility so that the proposed adaptive function (Eq. 4) could reproduce this waveform curve. According to the Eq. 7 parameter M mainly control the slope of temperature in the fusion line where ω is 1 Fig. 7 and Fig. 8 show the temperature curve along y-axis and x-axis on the upper surface of the plate of test No.2 with different values of M. As shown in Fig. 7 and Fig. 8 by changing the values of M temperature gradient can

be changed in the fusion line while the weld pool size and the maximum temperature do not change [4].

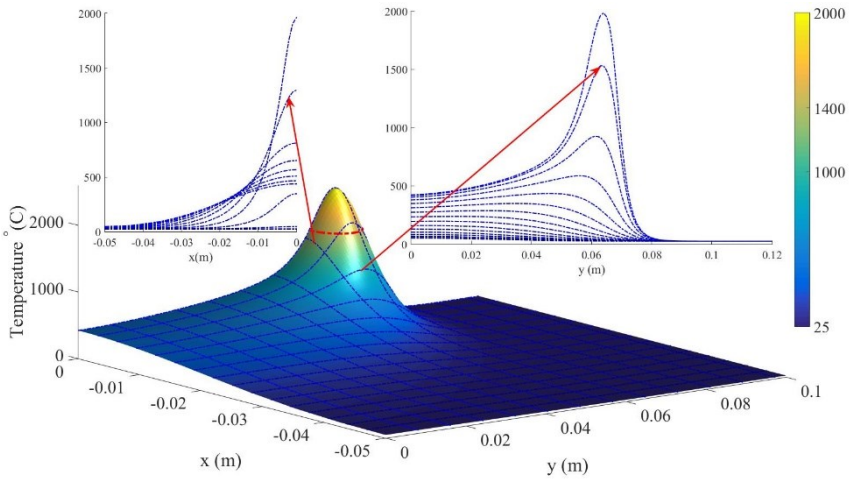

Fig. 6 Temperature distribution on the upper surface of the plate of test No.2 as calculated with the FEM and waveform curve cross section parallel to the x and y-axis

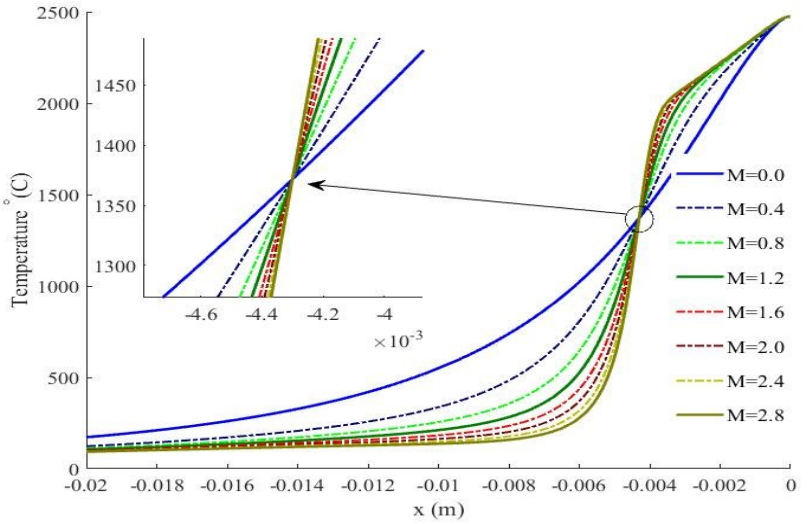

Fig. 7 Effect of parameter M on temperature curve along the x-axis at point ξ=0 on the upper surface of welding sample of the test No. 2

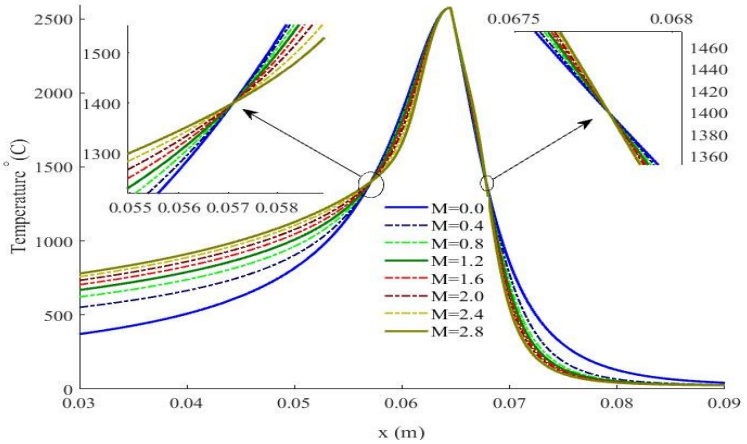

Fig. 8 Effect of parameter M on temperature curve along the y-axis at point x=0 on the upper surface of welding sample of the test No. 2

The temperature gradient can also be controlled by N in each direction of heat flow. For instance, as shown in Fig. 9, the temperature gradient of the rear part of the temperature curve changes by changing the N parameter in this direction (N_{yr}). The flexibility of the adaptive function to get matched to any curve with such configuration is provided by the parameters of the modification function (M, N_x, N_{yf}, N_{yr}, and N_z) each of which particularly affects a certain part of the temperature curve [4].

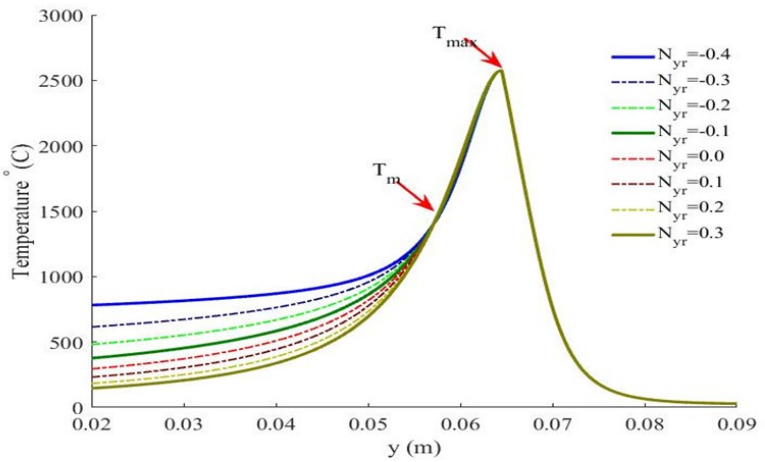

Fig. 9 effect of parameter Nyr on temperature curve along the y-axis at point x=0 on the upper surface of welding sample of the test No. 2

ESTIMATION OF THE PARAMETERS OF THE ADAPTIVE FUNCTION

The parameters of the adaptive function are classified into adaptive function parameters including a_m, b_m, c_m, d_m and B and parameters of the modification function including M, Nx, Nyf, Nyr and Nz. According to Eq. 8, the parameter B is a function of the heat diffusivity and welding speed. Since the heat diffusivity is a temperature dependent and it is not possible to consider variable material properties in an analytical solution, an optimum constant value is considered for the heat diffusivity of each welding material based on the estimated maximum temperature (Tmax) [4]. The parameters of a_m, b_m, c_m, d_m are determined according to the weld pool dimensions using Eq. 4. To compensate for the discrepancies between the results of the adaptive function and measured temperature, the parameters of the modification function are adjusted in such a way that the computation error is reduced. The M parameter is assumed to be constant and therefore the parameters of N_x, N_{yf}, N_{yr}, and N_z can vary by the dimensionless parameter of ω. A MatLab routine developed to estimate the optimum values of the parameters of the modification function according to the measured temperature in such a way that the computation error is reduced. The computation error is the relative error of the calculated temperature compared to the measured temperature based on a method proposed in [4]. Table 7 presents the constant parameters of the adaptive function for tests No.1-8. The maximum temperature of 2500 °C was assumed at the origin of the moving coordinate system and accordingly the estimated value of $\frac{\rho c}{2k}$ is $7571^{S}/_{m^2}$ and thus, the parameter B changes in accordance with the welding speed (v). The accuracy of the result of the adaptive function shows low sensitivity to the values of N_z and N_{yf}. Therefore, an optimum constant values were estimated for N_z and N_{yf}.

Table 7 Parameters of the adaptive function for test No. 1-8

Test No.	a_m	b_m	c_m	$d_m \times 10^{-4}$	$B = \frac{\rho c}{2k} v \ (1/m)$	M	N_z	N_{yf}
1	11.45	14.06	4.35	4.03	53.5	0.45	-0.44	0.45
2	11.02	12.09	3.71	3.92	63.6			
3	10.71	10.06	3.33	3.86	75.7			
4	11.23	8.51	3.27	3.96	90.8			
5	9.34	8.91	3.03	3.99				
6	14.13	15.69	4.44	3.94	63.6			
7	9.34	8.91	3.03	3.99				
8	11.02	12.09	3.71	3.92				

Fig. 10 shows the estimated N_x as a function of ω_x. As shown in Fig. 10 by increasing ω_x, the parameter N_x decreases. Eq. 10 is a proposed extrapolation function of N_x according to the ω_x. Fig. 11 shows the estimated values of N_{yr} as a function of ω_x and rear tail of the weld pool (L_r). Eq. 11 is a linear extrapolation function for N_{yr}.

$$N_x(\omega_x) = \frac{4.3}{{\omega_x}^2 + 0.61} + 0.015 \quad (10)$$

$$N_{yr}(\omega_x, L_r) = -4.7\omega_x \times L_r + 0.02\omega_x + 4.4Lr - 0.24 \quad (11)$$

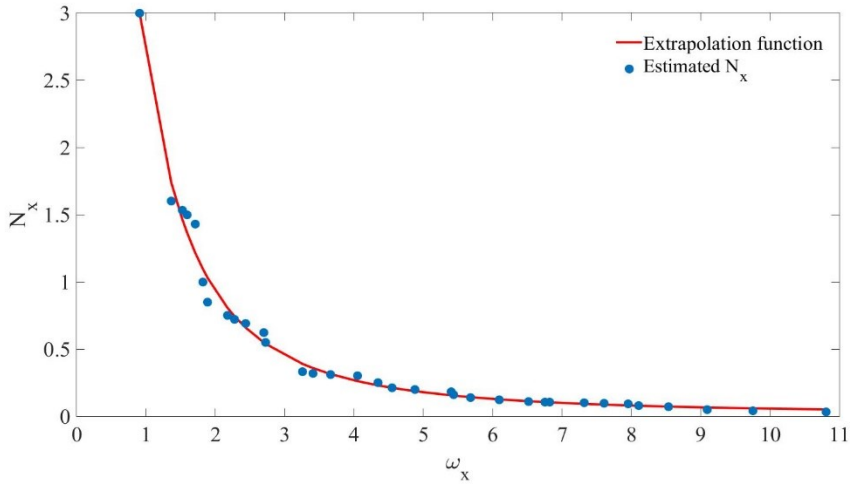

Fig. 10 Estimated N_x for test No. 1-4 as a function of ω_x and extrapolation function result (Eq. 10)

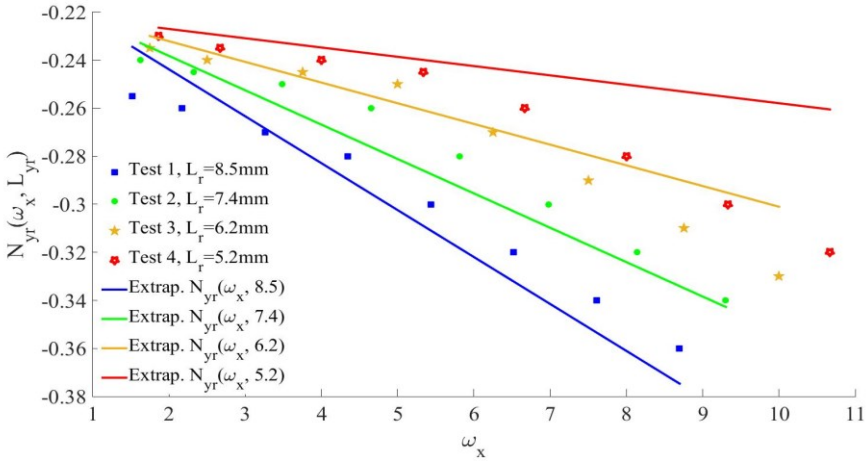

Fig. 11 Estimated N_{yr} for test No. 1-4 as a function of ω_x and L_r and extrapolation function result (Eq. 11)

ADAPTIVE FUNCTION RESULTS

RESULTS OF THE ADAPTIVE FUNCTION METHOD

Fig. 12 shows the temperature distribution on the upper surface of the welding plate of test No.1 calculated by the adaptive function. As shown in Fig. 12 the calculated fusion line by the adaptive function method matches to the measured fusion line quite well. The relative error of the calculated temperature rather than the measured temperature is between 5-9% while the relative error of the FEM in the case of the test No. 1 (Fig. 3) is 12-22% which shows almost 60% improvement. Fig. 13 and 14 show the temperature distribution on the upper surface of the plate of test No.2 calculated by FEM and adaptive function respectively. In the case of the test No. 2, the relative error of the adaptive function is less than 8% and the relative error of the FEM is more than 12%. It is worth noting that the computation cost including computation time, verification and data provisioning in case of the adaptive function is much less than the FEM which discussed in reference [4] with detail.

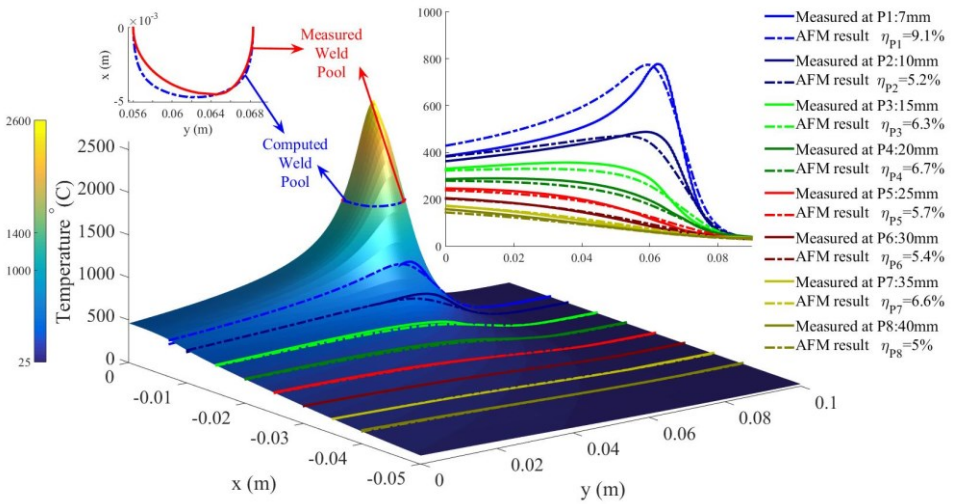

Fig. 12 Temperature distribution on the upper surface of the welding sample of test No. 1 as calculated with the adaptive function approach (welding speed 7 cm/min, welding current 150A)

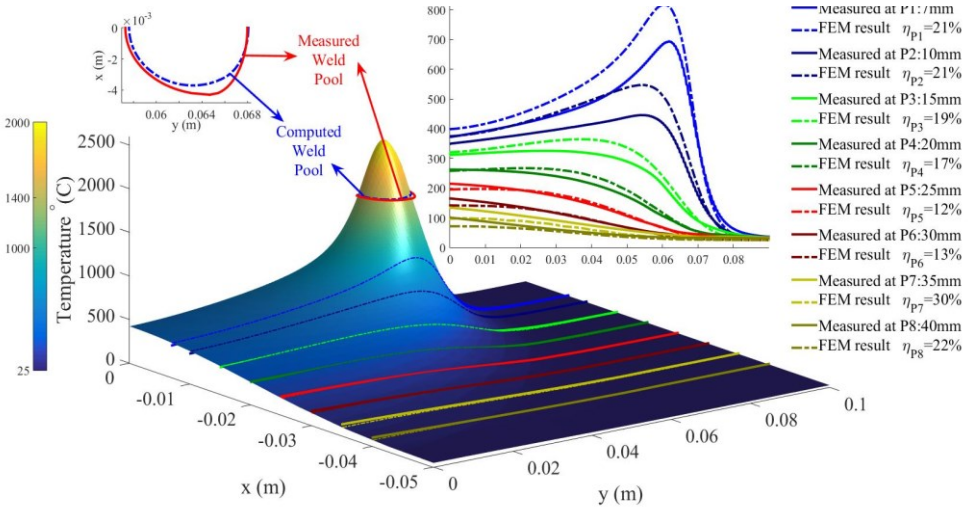

Fig. 13 Temperature distribution on the upper surface of the welding sample of test No. 2 as calculated with the FEM (welding speed: 8.4 cm/min, welding current: 150A)

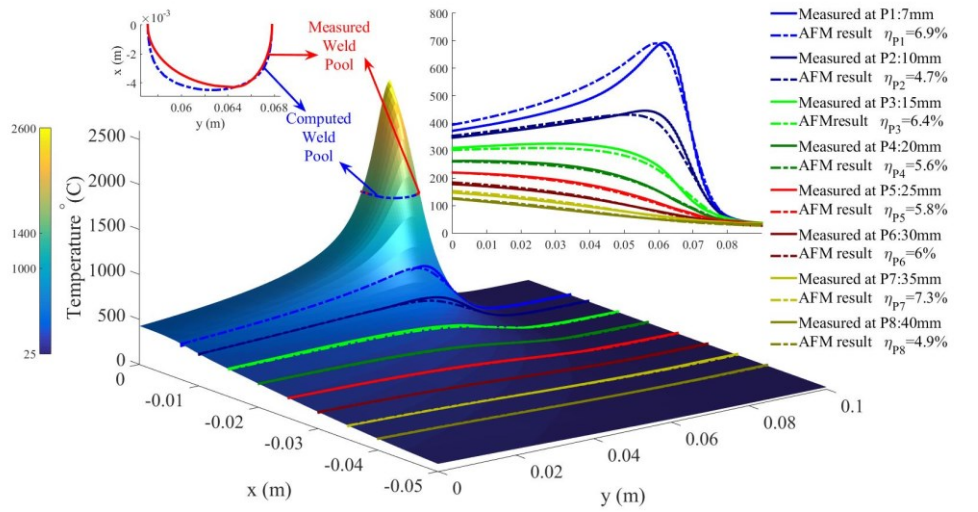

Fig. 14 Temperature distribution on the upper surface of the welding sample of test No. 2 as calculated with the adaptive function approach (welding speed:8.4 cm/min, welding current:150A)

WELDING SPEED EFFECT

Fig. 15-18 show the measured and calculated time-temperature curves at point 1-8 for tests No. 1-4. According to the Table 1, the welding speed for test No.1-4 are 7, 8.4, and 10 and, 12cm/min respectively, therefore the parameter B changes accordingly (Table 7). The constant parameters given in Table 7 and Eq. 10 and 11 were used as the parameters of the adaptive function. The overall relative error of 5.3, 4.9, 5.1, and 5.1% were calculated for tests No. 1-4 respectively which shows high accuracy of the adaptive function in different welding speed. As shown in Fig. 19 by increasing welding speed, heat input decreases and thus, the peak temperature decreases at the same measuring points.

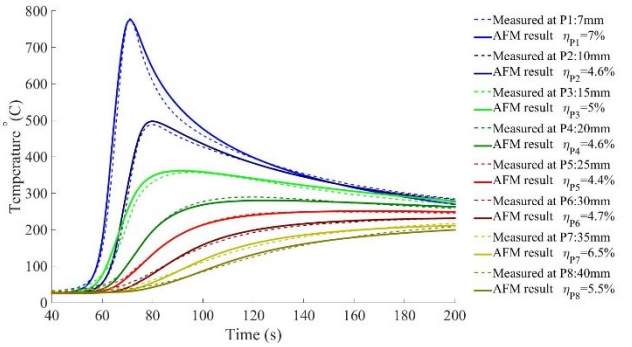

Fig. 15 Time-temperature curve measured and calculated by the adaptive function for test No.1 (speed: 7 cm/min)

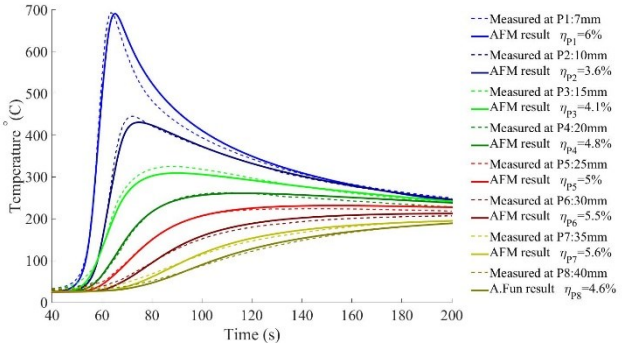

Fig. 16 Time-temperature curve measured and calculated by the adaptive function for test No.2 (speed: 8.4 cm/min)

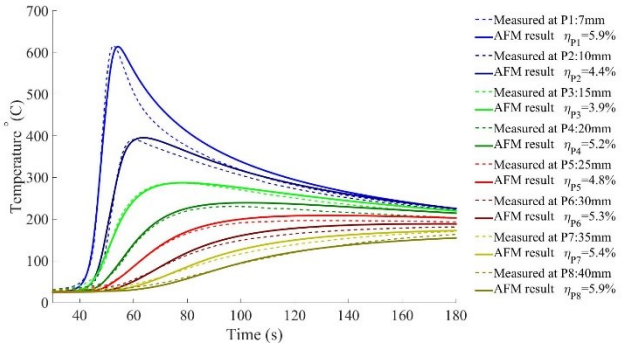

Fig. 17 Time-temperature curve measured and calculated by the adaptive function for test No.3 (speed: 10 cm/min)

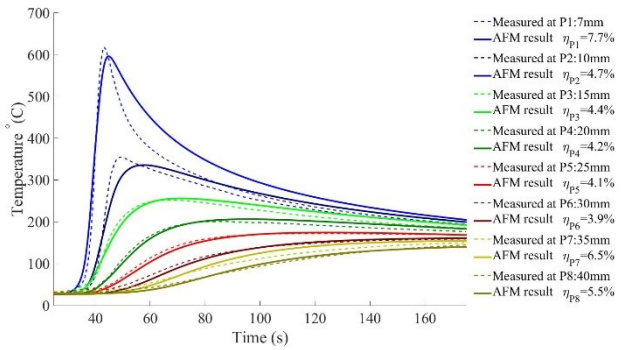

Fig. 18 Time-temperature curve measured and calculated by the adaptive function for test No.4 (speed 12 cm/min)

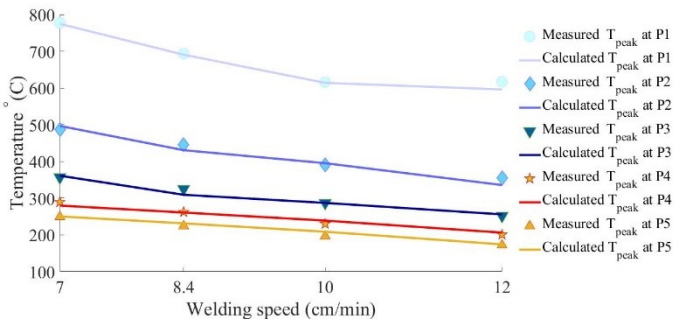

Fig. 19 Peak temperature of P1-P5 as a function of welding speed

WELDING CURRENT EFFECT

Fig. 21 and Fig. 21 show the measured and calculated time-temperature curves at point 1-8 for tests No. 5 and 6 with welding speed of 8.4 $\frac{cm}{min}$ and welding current of 125 and 175 A. The welding speed of test No. 2 is also 8.4 $\frac{cm}{min}$ while the welding current is 150 A. As shown in Fig. 20, Fig. 16 and Fig. 21 the adaptive function is able to predict temperature with a high accuracy of 5% using the constant parameters given Table 7 and Eq. 10 and 11 as extrapolation functions of N_x and $N_{yr.}$. As shown in Fig. 22 by increasing welding current, heat input increases and thus, the weld pool dimensions and peak temperature decrease at the same measuring points.

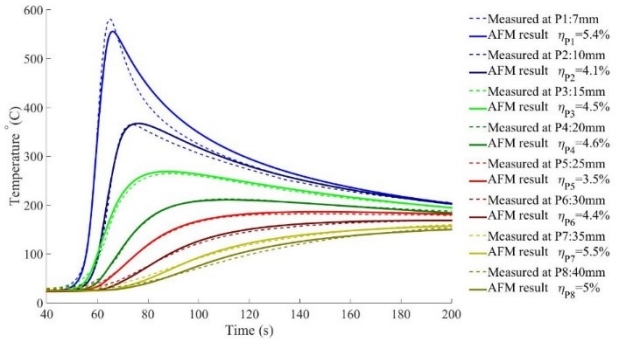

Fig. 20 Time-temperature curves measured and calculated by the adaptive function for test No.5 (welding current 125A)

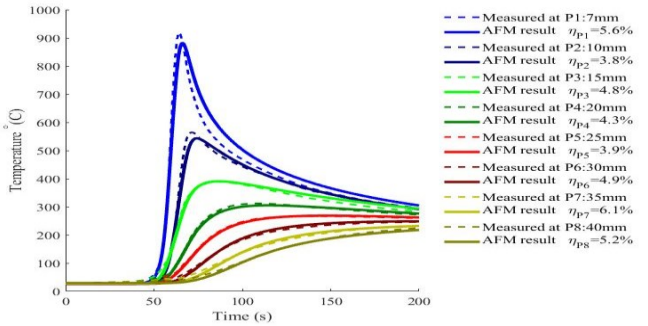

Fig. 21 Time-temperature curves measured and calculated by the adaptive function for test No. 6 (welding current 175A)

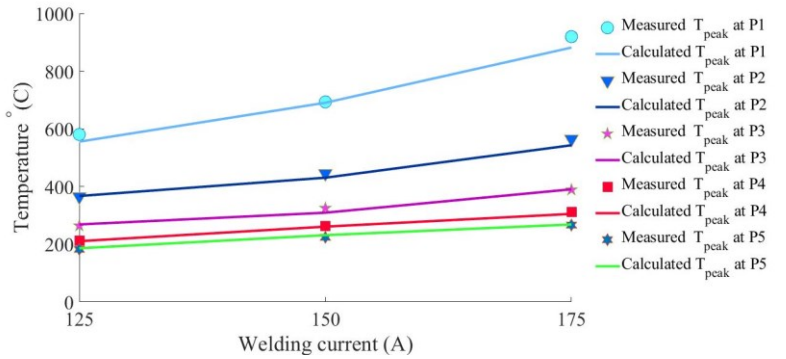

Fig. 22 Peak temperature of P1-P5 as a function of welding current

Fig. 23 and 24 show the result of the adaptive function for test No.7 and 8. The welding parameters of test No.7 and 8 are the same as test No. 5 and 2 respectively but the temperature measurement has been done on the bottom surface. The result indicates that a constant value of Nz equal to -0.44 provides a good agreement between the adaptive function and measured temperature.

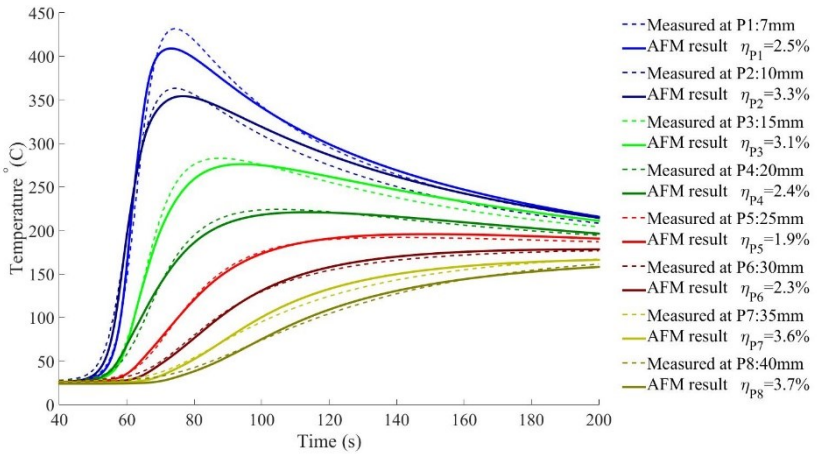

Fig. 23 Time-temperature curves measured and calculated by the adaptive function for test No.7 (welding current 125A), thermocouples installed on the beneath of the plate

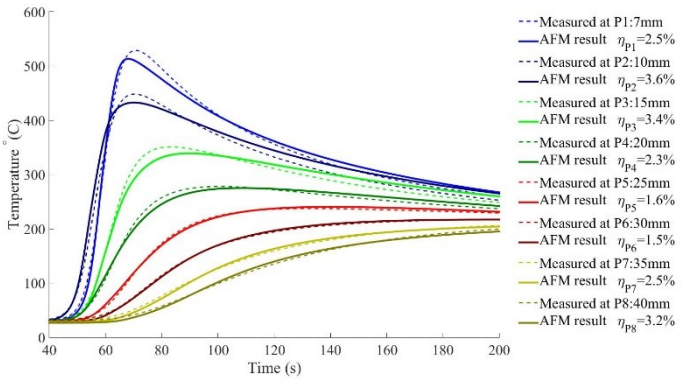

Fig. 24 Time-temperature curves measured and calculated by the adaptive function for test No.8 (welding current 150A), thermocouples installed on the beneath of the plate

CONCLUSION

In this paper, the new analytical model called “adaptive function method” (AFM) was applied to study the welding temperature distribution in different welding circumstances and a correlation between welding circumstance and the parameters of the adaptive function was developed. The heat flow problem in welding with various welding current and speed were solved by Rosenthal’s method, FEM, and the adaptive function method and the accuracy of the models compared. The results can be summarized as follows:

- The accuracy of the adaptive function is much higher than the other methods in all studied cases. The relative error of the adaptive function is almost 5% which is not comparable with FEM and Rosenthal’s approach.
- The parameters of the adaptive function are expressed as a function of a dimensionless parameter of ω and L_{yr} (the rear tail of the weld pool). The weld pool dimension and dimensionless parameter can be expressed as a function of welding speed and current.

The adaptive function method is an effective solution to heat flow problem in welding with the most accurate result and low computation cost. Accordingly, the following advantages of the adaptive function method are expected:

- Since temperature calculation does not require meshing, the calculated temperature gradient helps us to develop an automatic adaptive meshing algorithm to apply in the mechanical simulation of welding.
- The parameters of the adaptive function are directly determined by temperature measurement and no information about material properties, phase transformation, and heat source parameters are required.

REFERENCESV

[1] K. MASUBUCHI, Heat flow in weldments, in: Anal. Welded Struct., Elsevier, 1980: pp. 60–87.

[2] T.W. EAGAR, N.S. TSAI, Temperature fields produced by traveling distributed heat sources, Weld. J. 62 (1983) 346–355.

[3] L.-E. LINDGREN, Finite Element Modeling and Simulation of Welding Part 1 :, J. Therm. Stress. 24 (2012) 141–192.

[4] M.B. NASIRI, N. ENZINGER, Powerful analytical solution to heat flow problem in welding, Int. J. Therm. Sci. 135 (2019) 601–612. doi:10.1016/j.ijthermalsci.2018.08.003.

[5] D. ROSENTHAL, The Theory of Moving Source of Heat and its Application to Metal Transfer, ASME Trans. 43 (1946) 849–866.

[6] M.B. NASIRI, M. BEHZADINEJAD, H. LATIFI, J. MARTIKAINEN, Investigation on the influence of various welding parameters on the arc thermal efficiency of the GTAW process by calorimetric method, J. Mech. Sci. Technol. 28 (2014). doi:10.1007/s12206-014-0736-8.

[7] W. ZHANG, T. DEBROY, T.A. PALMER, J.W. ELMER, Modeling of ferrite formation in a duplex stainless steel weld considering non-uniform starting microstructure, Acta Mater. 53 (2005) 4441–4453.

[8] J.J. DEL COZ DÍAZ, P. MENÉNDEZ RODRÍGUEZ, P.J. GARCÍA NIETO, D. CASTRO-FRESNO, Comparative analysis of TIG welding distortions between austenitic and duplex stainless steels by FEM, Appl. Therm. Eng. 30 (2010) 2448–2459.

[9] SYSTUS 2017: Reference Analaysis Manual, ESI Group., 2017.

[10] J. GOLDAK, A. CHAKRAVARTI, M. BIBBY, A new finite element model for welding heat sources, Metall. Trans. B. 15 (1984) 299–305.

[11] C.M. ADAMS JR, Cooling rates and peak temperatures in fusion welding, Weld. J. 37 (1958) 210s–215s.

[12] N. CHRISTENSEN, V. DAVIES, K. GJERMUNDSEN, Distribution of temperatures in arc welding, Br. Weld. J. 12 (1965) 54–75.

[13] R. KOMANDURI, Z.B. HOU, Thermal analysis of the arc welding process: Part I. General solutions, Metall. Mater. Trans. B. 31 (2000) 1353–1370.

[14] N.T.NGUYEN, A.OHTA, K.MATSUOKA, N.SUZUKI, Y.MAEDA, Analytical Solutions for Transient Temperature of Semi-Infinite Body Subjected to 3-D Moving Heat Sources, Weld. Res. Suppl. I (1999) 265–274.

[15] S.K. JEONG, H.S. CHO, An analytical solution to predict the transient temperature distribution in fillet arc welds, Weld. Journal-Including Weld. Res. Suppl. 76 (1997) 223s.

[16] A.S. AZAR, S.K. AS, O.M. AKSELSEN, Determination of welding heat source parameters from actual bead shape, Comput. Mater. Sci. 54 (2012) 176–182.

[17] L.-E. LINDGREN, Finite Element Modeling and Simulation of Welding. Part 2: Improved Material Modeling, J. Therm. Stress. 24 (2001) 195–231.